


RESEARCH ARTICLE

Overlapping but distinct TDP-43 and tau pathologic patterns in aged hippocampiVanessa D. Smith¹, Adam D. Bachstetter^{2,3}, Eseosa Ighodaro^{3,4}, Kelly Roberts², Erin L. Abner^{4,5}, David W. Fardo⁶, Peter T. Nelson ^{1,3,4}¹ Department of Pathology and Laboratory Medicine, ² Spinal Cord and Brain Injury Research Center, ³ Department of Neuroscience, ⁴ Sanders Brown Center on Aging, ⁵ Department of Epidemiology, ⁶ Department of Biostatistics, University of Kentucky, Lexington, KY.**Keywords**

colocalization, FTLN, hippocampal sclerosis, hippocampus, HS-aging, oldest-old.

Corresponding author:Peter T. Nelson, MD, PhD, University of Kentucky, Sanders-Brown Center on Aging, 800 S. Limestone, Rm 311, Lexington, KY 40536-0230 (E-mail: pnels2@email.uky.edu)

Received 6 January 2017

Accepted 6 March 2017

Published Online Article Accepted

9 March 2017

doi:10.1111/bpa.12505

Abstract

Intracellular proteinaceous aggregates (inclusion bodies) are almost always detectable at autopsy in brains of elderly individuals. Inclusion bodies composed of TDP-43 and tau proteins often coexist in the same brain, and each of these pathologic biomarkers is associated independently with cognitive impairment. However, uncertainties remain about how the presence and neuroanatomical distribution of inclusion bodies correlate with underlying diseases including Alzheimer's disease (AD). To address this knowledge gap, we analyzed data from the University of Kentucky AD Center autopsy series (n = 247); none of the brains had frontotemporal lobar degeneration. A specific question for this study was whether neurofibrillary tangle (NFT) pathology outside of the Braak NFT staging scheme is characteristic of brains with TDP-43 pathology but lacking AD, that is those with cerebral age-related TDP-43 with sclerosis (CARTS). We also tested whether TDP-43 pathology is associated with comorbid AD pathology, and whether argyrophilic grains are relatively likely to be present in cases with, vs. without, TDP-43 pathology. Consistent with prior studies, hippocampal TDP-43 pathology was associated with advanced AD – Braak NFT stages V/VI. However, argyrophilic grain pathology was not more common in cases with TDP-43 pathology in this data set. In brains with CARTS (TDP-43[+]/AD[–] cases), there were more NFTs in dentate granule neurons than were seen in TDP-43[–]/AD[–] cases. These dentate granule cell NFTs could provide a proxy indicator of CARTS pathology in cases lacking substantial AD pathology. Immunofluorescent experiments in a subsample of cases found that, in both advanced AD and CARTS, approximately 1% of dentate granule neurons were PHF-1 immunopositive, whereas ~25% of TDP-43 positive cells showed colocalized PHF-1 immunoreactivity. We conclude that NFTs in hippocampal dentate granule neurons are often present in CARTS, and TDP-43 pathology may be secondary to or occurring in parallel with tauopathy.

INTRODUCTION

Transactive response DNA binding protein 43 (TDP-43) inclusion bodies, detected with immunohistochemistry, are a pathologic biomarker discovered in studies of the disease spectrum that includes amyotrophic lateral sclerosis (ALS) and frontotemporal lobar degeneration (FTLD) (61). Since that discovery, TDP-43 inclusion bodies have also been described in a diverse group of neurodegenerative, developmental, and neoplastic conditions (60). These findings are conceptually similar to results from separate studies that revealed tau protein inclusion bodies in many different human brain diseases (“tauopathies”) (1, 73). The manifestation of TDP-43 and/or tau protein aggregates in numerous diseases indicates that diverse upstream factors can lead to common downstream proteinopathies; the inclusion bodies may be both “reactive” and harmful in their own right (26, 29, 43, 60).

TDP-43 and tau pathologies often coexist in the same brain. Chronic traumatic encephalopathy is an example of a progressive neurodegenerative condition in which a well-documented upstream initiator (repetitive brain trauma) may trigger both TDP-43 and tau neurofibrillary tangle (NFT) pathologies (49, 70). It has also been reported that TDP-43 pathology is associated with comorbid tau-immunoreactive argyrophilic grain (AG) pathology (5), which provides evidence of a different cause of coexisting tau and TDP-43 pathologies. It is not known if tau and TDP-43 pathologies are initiated and/or exacerbated by: (i) environmental or genetic “upstream” pathogenic initiator(s); (ii) age-related biological mechanism(s), for example impaired protein degradation; (iii) pathological “seeding” or some other synergistic mechanism(s); or (iv) some combination of the above.

Yet another brain condition characterized by abnormal proteostasis is Alzheimer's disease (AD). The hallmark features of AD are

NFTs and amyloid- β (A β) amyloid plaques (53). TDP-43 pathology is a frequent comorbidity in brains with AD, and TDP-43 pathology is associated with more severe cognitive impairment than would be expected for given levels of amyloid plaques and NFTs (17, 33, 36, 48, 54, 55, 77).

While AD is a common cause of dementia, there are other prevalent diseases that are often misdiagnosed as AD in the clinical setting due to overlapping symptoms. For example, in many individuals diagnosed as “Probable AD” during life according to the McKhann diagnostic criteria (50), autopsy often instead reveals both hippocampal sclerosis (HS) and comorbid TDP-43 pathologies (10, 63). Terms previously used to describe these cases include HS-Aging, HpScl, and HS dementia (11, 19, 46, 59, 83) which describe a disease clinically and pathologically distinct from either AD or FTLD (2, 10, 58, 60). Because the current terminology was unsatisfactory (see Discussion), we proposed a new descriptive designation: “Cerebral age-related TDP-43 with sclerosis” (CARTS) (60). This term reflects that the disease preferentially affects persons in advanced old age and TDP-43 pathology is a relatively specific marker that could precede full-blown HS. Although not universally applied currently, this diagnostic term has been practically useful in both clinical/diagnostic (15) and research (60) contexts.

We previously described a case with CARTS pathology and comorbid NFTs in a neuroanatomic distribution that diverged from the Braak NFT staging system, specifically in hippocampal dentate granule neurons (7). Prior studies focused on TDP-43 pathology in cases with AD (16, 33, 34, 78), and other studies reported that a subset of cells have colocalized tau, TDP-43, and/or HS pathologies (3, 7, 16, 25, 38, 41, 51, 81). However, detailed description of the hippocampal tau pathology seen in CARTS is lacking in the literature.

The goal of this study was to analyze the relationship between common TDP-43 and tau pathologies in aged human brains. Specifically, we examined whether CARTS pathology, in cases lacking AD, is associated with tau pathology – NFTs and/or AGs. Data were analyzed from the University of Kentucky Alzheimer’s Disease Center (UK-ADC) autopsy series with detailed neuropathological observations ($n = 247$ that were stained immunohistochemically for TDP-43). Our study indicates that there are at least two common patterns of TDP-43 and tau protein misfolding in human brain aging. In patients lacking substantial AD pathology, CARTS cases tend to have tau NFTs in the hippocampal dentate granule neurons, providing a potential proxy indicator of CARTS.

MATERIALS AND METHODS

Clinical cohort and neuropathological assessments

All protocols were performed with approval from the University of Kentucky Institutional Review Board. Details of recruitment, inclusion/exclusion criteria, clinical assessments, and neuropathological protocols have been described elsewhere (57, 72). Two-hundred and forty-seven cases were included representing a convenience sample of those with available TDP-43 immunohistochemical staining, which started to be routinely performed in 2009. Pathological assessments were performed at the UK-ADC using methodology that was described previously including Gallyas silver staining (18, 57, 67, 80). Patients with relatively rare dementia syndromes

(eg prions, trinucleotide repeat diseases, or FTLD), or any brain tumor were excluded. FTLD cases are uncommon in this cohort as they are in other community-based samples; the included cases lacked clinical FTD symptoms (aphasic or behavioral variants) and the AD–/TDP-43+ cases met inclusion criteria for CARTS, that is died age >85 years of age with limited distribution of TDP-43 pathology.

Immunohistochemical stains for phosphorylated tau, PHF-1 (gift from Dr. Peter Davies; 1:500 dilution), phospho-TDP-43 (1D3 clone, gift from Dr. Manuela Neumann, 1:500 dilution), and amyloid- β (Vector Laboratories, Burlingame, CA, USA; 1:100 dilution) were used to assess NFTs, neuritic amyloid plaques, TDP-43 pathology, and A β plaques on brightfield microscopy, following the National Institute on Aging-Alzheimer’s Association (NIA-AA) consensus recommendations (27).

TDP-43 pathology refers to immunohistochemical staining that was neuritic, intranuclear, cytoplasmic, or otherwise tangle- or thread-like. Severity of TDP-43 pathology was graded in immunostained hippocampal sections (left side) using a 0–2 semiquantitative scale, with 1 representing minimal pathology. A case with minimal dentate granule neuron TDP-43 pathology would be scored as at least a 1 on this scale. Tau pathology was graded based on Braak NFT staging with complementary quantitative counts being performed as described below. AG pathology was graded on a 0–3 scale in multiple medial temporal lobe regions as described previously (55).

We tested specifically whether there was an association between CARTS and tau tangle pathology in the dentate gyrus, because we previously observed NFTs in dentate granule neurons in CARTS cases with Braak NFT stages $<III$ (8). This is a deviation from the Braak NFT staging scheme wherein “a few” phospho-Tau immunoreactive tangles appear in Braak NFT Stage IV and more are seen in Stages V and VI (8). A convenience sample of cases was used with known AD status (Braak NFT Stages 0–II vs. Stages V/VI) and known TDP-43 pathology status for the purpose of correlating TDP-43 pathology and dentate granule neuron NFTs, focusing on the CARTS (TDP-43[+]/AD[–]) cases. For this sample, the AD cases also had moderate or severely dense neuritic amyloid plaques according to CERAD criteria (52). A neuropathologist (VDS) blinded to AD and TDP-43 status manually scored PHF-1 staining in the dentate gyrus. The lengths of the dentate granule cell layers were measured and NFT counts adjusted based on dentate gyrus length.

Immunofluorescence sample processing

Immunofluorescent staining was performed using methods previously described (6). Sections cut at 8 μ m thickness were deparaffinized prior to microwave antigen retrieval for 6 min (power 8) using citrate buffer (Declere buffer, Cell Marque; Rocklin, CA, USA). The sections were then placed in 100% formic acid for 3 min. Sections were blocked in 5% normal goat serum in Tris buffered saline (5% NGS + TBS) for 1 h at room temperature, then incubated in primary antibodies (PHF-1 at 1:500 and ID3 was used at 1:50 for immunofluorescence), diluted in 5% NGS + TBS, for 22 h at 4°C. Secondary antibodies were conjugated to an Alexafluor probes (1:200, Cat nos. A11007 and A21121, Life Technologies; Carlsbad, CA) diluted in 5% NGS + TBS for 1 h at 19–22°C. Sections were then incubated for 10 min at 19–22°C in a 0.1% solution

of Sudan Black (Sigma, cat no. 199664) prepared in 70% ethanol, to reduce autofluorescence. Slides were coverslipped using Vectashield mounting medium with DAPI (cat no. H-1200, Vector Labs, Burlingame, CA, USA). To determine the threshold of pixel intensity of real staining over background autofluorescence, a positive control case known to have high P-TDP-43 and PHF-1 staining in the dentate gyrus was used. As technical controls, slides were stained with P-TDP-43 only, PHF-1 only, neither primary antibody, or with both P-TDP-43 and PHF-1 to demonstrate specificity. For experimental cases, two sections from each case were stained with P-TDP-43 and PHF-1. Three AD cases (all Braak NFT stage V) and three CARTS cases (all Braak NFT stage II), all known to have TDP-43 pathology, were included in the analysis. Images were acquired on a Nikon C2Plus Confocal Microscope, using a Plan Fluor 40× Oil (1.3 NA) objective, a pinhole of 1.2 airy unit (AU), step size of 1 μm, and an image size of 512 × 512, with a 1× zoom, using a channel series scan. Non-overlapping images of the entire granular cell layer of the dentate gyrus were acquired for each of the two sections for each of the cases. Images that had at least one PHF-1 or P-TDP-43 immunoreactive profile were included in the analysis.

To determine the percentages of PHF-1 and TDP-43 colocalization, Imaris 3D microscopic data analysis software was used (version 8.3 Bitplane USA Concord, MA, USA). Using images acquired with slides stained for PHF-1 only or P-TDP-43 only we determined the threshold where positive staining could be detected without detecting background. Using these settings in the Imaris Coloc function, a new image channel was created corresponding to the colocalized pixels. A standardized LUT setting was used for viewing the images for each channel (DAPI, PHF-1, P-TDP-43, and colocalized). A surface reconstruction was made to provide an unbiased digital quantification of the number of PHF-1+ NFTs and the number of TDP-43+ inclusions. Settings for the surface reconstruction included a size limitation for the PHF-1 staining, so small neurites would not be included in the count of the number of positive cells. All settings for the surface reconstruction were held constant for all the images acquired. After the surfaces were rendered, an observer would count the number of rendered NFTs (PHF-1) or inclusions (P-TDP-43). The observer then determined if there was a colocalized signal in those 3D rendered objects. The total number of neurons in the image was determined using the Imaris spot detection of DAPI positive cells, focused primarily upon the granular cell layer of the dentate gyrus.

Data analysis

Statistical analyses were carried out using the JMP statistical software package (SAS version 9.1.3; SAS Institute, Inc., Cary, NC, USA). Descriptive statistics were used to describe the cohort. Continuous variables were summarized with means and standard deviations, or with median values and interquartile ranges (IQR), as appropriate. Categorical variables were summarized with counts and percentages. Associations of TDP-43 immunostaining and Braak NFT staging were assessed utilizing a proportional odds model. The proportional odds assumption was assessed with a score test. Association of TDP-43 status (present or absent) with entorhinal AG severity was assessed utilizing a Chi-square test. Quantification of PHF-1 immunoreactive tangles was adjusted for dentate granule length and compared as functions of both Braak NFT

Table 1. Neuropathological cohort by TDP-43 status.

	TDP-43 severity (0–2)		
	0	1	2
Average age of death (years)	87.76	87.88	89.69
Number of cases	156	17	74

staging (0–II vs. V/VI) and TDP-43 pathology (present or absent; for this comparison, only TDP-43 pathology with ordinal severity value of 2 were used). All statistical tests were 2-sided, and a *P*-value of less than 0.05 was considered statistically significant.

RESULTS

The average age of death of included subjects (n = 247) was 88.4 years, and most of the research volunteers were cognitively normal at intake and followed longitudinally as previously described (45, 58) – average MMSE score at intake was 25.8, average final MMSE score before death was 19.9. At autopsy, 63% of cases had TDP-43 grade of 0 (no staining detected), 6.9% with a grade of 1 (minimal staining) and 30% with a grade of 2 (Table 1).

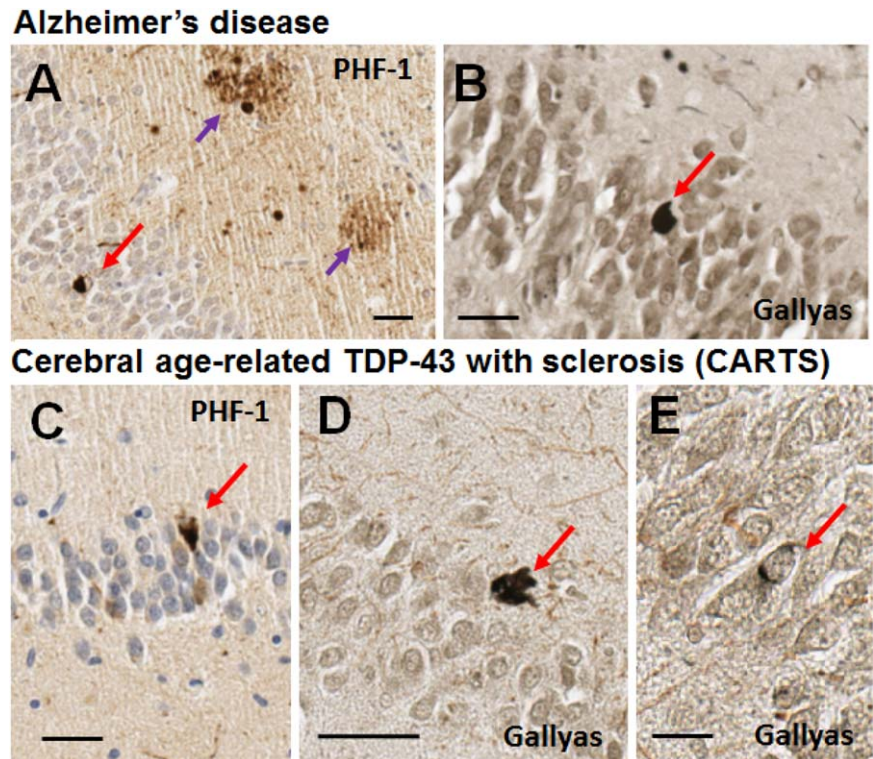
There was a marked tendency for cases with Braak NFT stages of V and VI to have TDP-43 pathology. In the overall sample, 46% of the brains had advanced AD with Braak NFT Stage V or VI, whereas 68% of TDP-43 grade 2 cases were Braak NFT Stage V or VI. Ordinal regression analysis demonstrated that the presence of TDP-43 was associated with a 2.76 fold (95% confidence interval (CI), 1.72 to 4.43) increased odds of having a more severe Braak stage (*P* = 2.5 × 10⁻⁵) (Table 2). In both AD and CARTS cases, NFTs in the dentate granule neurons could be stained with both PHF-1 and Gallyas silver stain (Figure 1), although the Gallyas silver stain appeared less sensitive as expected.

We tested whether AG pathology was associated with CARTS because AGs were previously shown to be associated with comorbid TDP-43 pathology (5, 25). In the UK-ADC sample, the distribution of AG severity was not statistically different for cases with vs. without TDP-43 pathology in the entorhinal cortex, subiculum, or CA1 region of the hippocampal formation (Table 3). When the cases with AGs (n = 43) were combined, this group was not more likely to have TDP-43 pathology in comparison with cases that lacked AG pathology (n = 197).

Table 2. Number of cases stratified by Braak NFT Stages and TDP-43 pathology.

Braak NFT stage	TDP-43 severity (0–2)		
	Absent	Present	
		0	1
0	2	0	4
I	19	2	3
II	37	3	5
III	21	3	5
IV	22	1	7
V	29	4	20
VI	26	4	30

Figure 1. Brightfield photomicrographs depict representative PHF-1 immunohistochemistry for phospho-tau (A,C) and Gallyas silver stain (B,D,E) in dentate granule neurons in Alzheimer’s disease and CARTS. The Alzheimer’s disease case (A,B) was a male with APOE ε 3/4 alleles, who died at age 85. Neuropathology showed Braak NFT Stage VI with CERAD neuritic plaque score of “moderate”. No TDP-43 pathology was observed. The CARTS case (C,D,E) was a female with APOE ε 2/3 alleles, who died at age 90. Thal Aβ stage was 1 (very few neocortical plaques detected with Aβ immunohistochemistry), CERAD neuritic plaque score of “none”, and Braak NFT stage I. There was substantial TDP-43 pathology in the hippocampus and subiculum. In both cases, NFTs were detected in dentate granule neurons with PHF-1 antibody, and with the Gallyas silver impregnation technique. Some of the NFTs stained with silver impregnation were dark fibrillar NFTs (D) whereas some were more subtle (E). Red arrows show NFTs, purple arrows show tau-positive neuritic plaques. Scale bar = 30 μM (A,B), 40 μM (C), 50 μM (D), and 15 μM (E).



We next addressed whether there was an increase in dentate granule PHF-1 immunoreactive NFTs in CARTS cases. By definition, CARTS cases show TDP-43 pathology but are not Braak NFT Stages V or VI (60). The rationales for that definition included that secondary protein misfolding has been found in advanced AD and TDP-43 specifically has been observed in that context (see Discussion). In a convenience subsample (Table 4) of individuals with previously ascertained hippocampal TDP-43 status and either Braak NFT Stages 0–II (n = 25) or Braak NFT Stages V/VI (n = 26), there were no detected differences in average CERAD neuritic plaque scores comparing those with and without TDP-43 pathology (Table 5). However, among cases with Braak NFT stages 0–II, but not Braak NFT stages V/VI, PHF-1 immunoreactive NFTs were more numerous in cases with TDP-43 pathology (CARTS cases) than in TDP[–] cases ($P < 0.05$) (Table 6).

Table 3. Number of cases stratified by argyrophilic grains (AGs) and TDP-43 pathology.

Entorhinal AGs	TDP-43 status (number of cases)		
	Absent	Present	
	0	1	2
0	118	14	65
1	16	1	5
2	10	1	2
3	5	1	2

We tested whether the same neurons in the fascia dentata of the hippocampus were immunopositive for both TDP-43 pathology and phospho-tau tangles, using double-label immunofluorescence; Figure 2 shows representative results in both AD and CARTS cases. We analyzed a convenience subsample of 6 cases that were immunopositive for TDP-43 pathology: 3 Braak NFT stage II, and 3 Braak NFT stage V, evaluating 2 different slides from each. Figure 3 helps to convey the cell counting and colocalization methods. The analyses included assessment of 14,200 dentate granule neurons from CARTS cases (among which were 74 PHF-1[+] cells and 165 TDP[+] cells), and 11,952 cells from AD cases (150 PHF-1[+], 171 TDP[+]). Whereas fewer than 2% of the dentate granule neurons in both AD and CARTS cases were immunopositive for either phospho-tau or TDP-43 pathology, there was a tendency for the pathologies to colocalize (Figure 4). The TDP-43 immunopositive dentate granule neurons were more likely to also contain tau tangles, in comparison with the percentage of PHF-1 immunoreactive cells in which TDP-43 pathology was detected (Figure 4C; $P = 0.007$).

Table 4. Convenience sample for assessing dentate granule NFTs stratified by TDP-43 status; shown are number of cases (avg. age of death), CARTS cases highlighted in yellow.

TDP-43 pathology severity	Braak 0–II N (mean age)	Braak V/VI N (mean age)
0	14 (90.1)	12 (87.9)
2	11 (90.3)	14 (89.1)

Table 5. Neuritic plaque pathology: shown are mean CERAD Scores, by TDP-43 pathology and Braak NFT Stage; CARTS cases highlighted in yellow.

Average CERAD neuritic plaque score (0–3)		
TDP-43 pathology severity	Braak 0–II	Braak V/VI
0	0.36	2.8
2	0.27	2.8

Table 6. Average number of PHF-1 immunoreactive dentate granule NFTs by TDP-43 pathology and Braak NFT Stage; CARTS cases highlighted in yellow.

Average # dentate granule NFTs (corrected for dentate length)		
TDP-43 pathology severity	Braak 0–II	Braak V/VI
0	0.42	9.5
2	4.2*	11.7

* $P < 0.05$ comparing TDP-43 0 vs. 2.

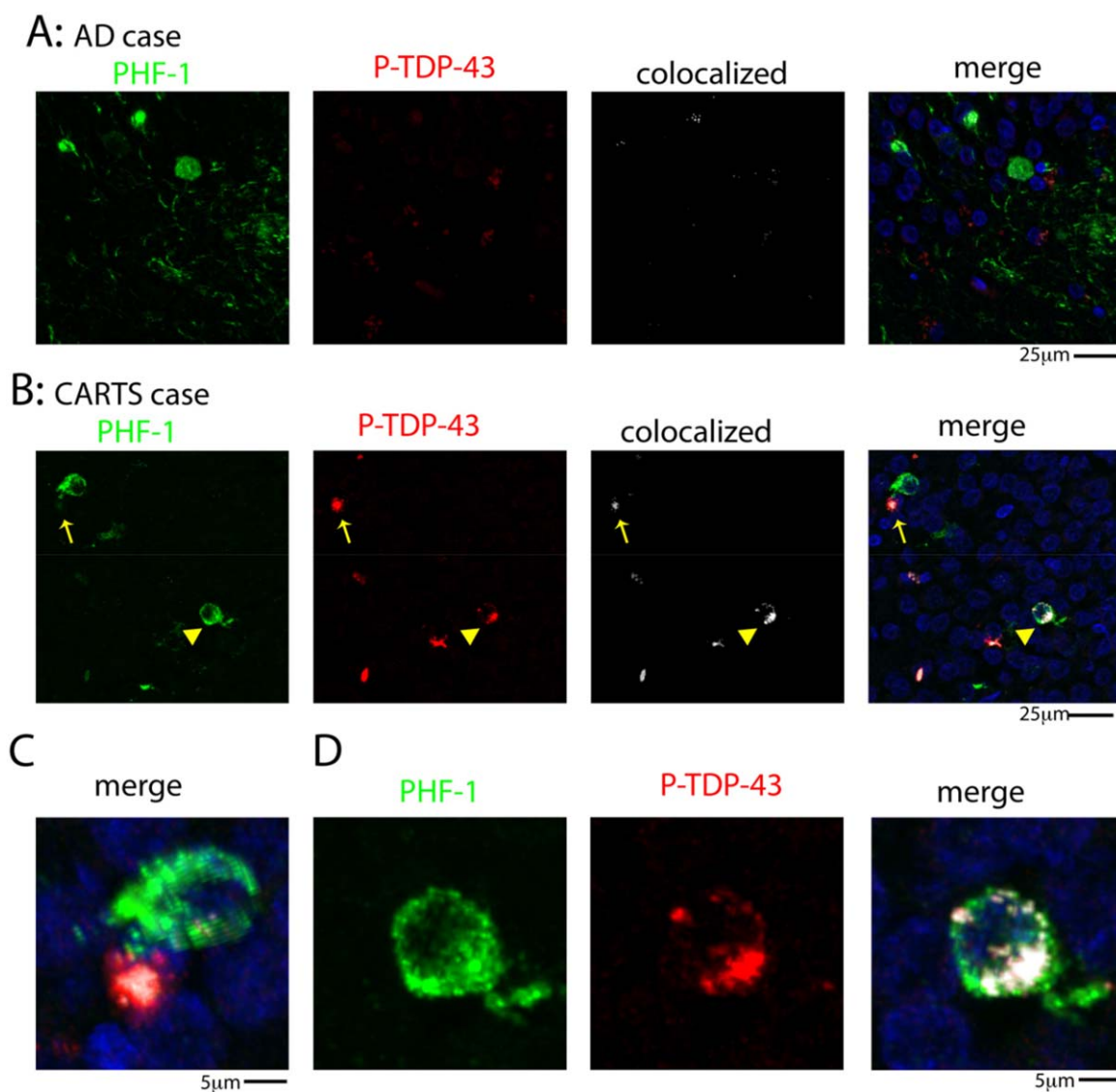


Figure 2. Double-label immunofluorescent images for tau (PHF-1) tangles and P-TDP-43 pathology in hippocampal dentate granule neurons. Representative examples are shown of PHF-1 and P-TDP-43 staining in an AD case (A) and a CARTS case (B). Arrow in (B) shows a P-TDP-43 inclusion in higher magnification in the merged

photomicrograph indicating the PHF-1 (green) and P-TDP-43 (red) signals are not colocalized (C). By contrast, the arrowhead in (B) shows a PHF-1 positive cell that is colocalized with P-TDP-43, as shown at a higher magnification in (D).

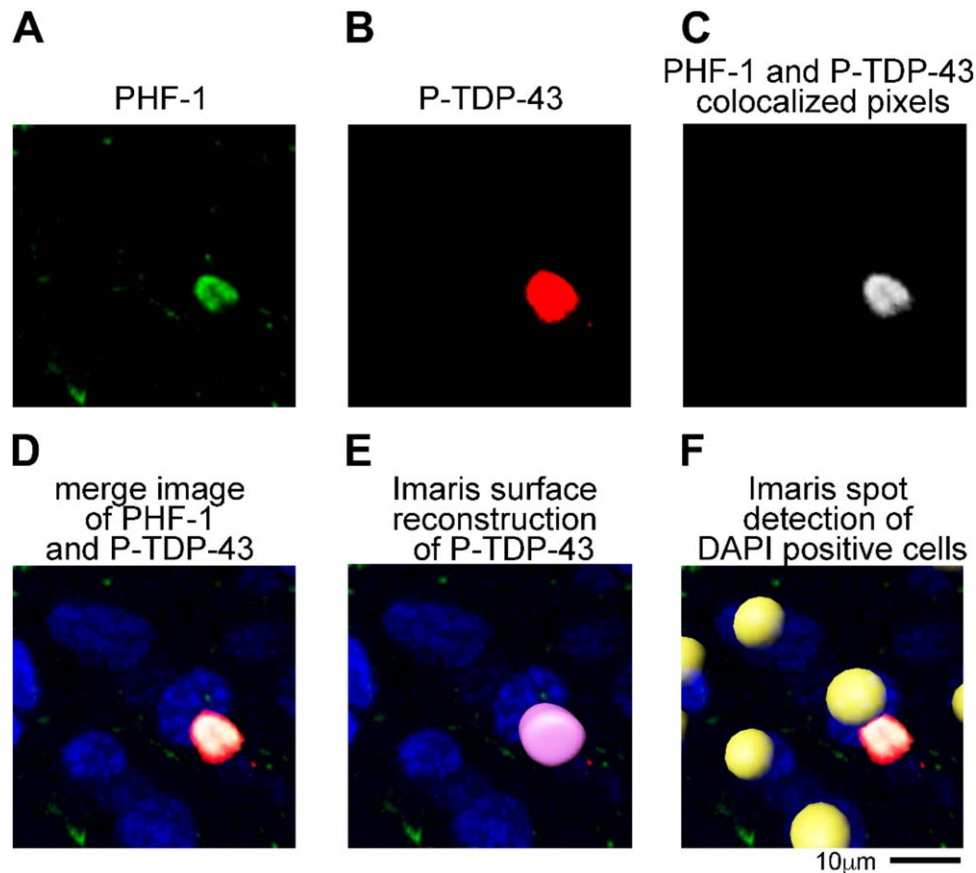


Figure 3. Cell counting and colocalization method used Imaris 3D microscopic data analysis software on confocal Z-stack images. **(A)** PHF-1 was thresholded to exclude pixels detected in the no PHF-1 primary antibody control samples. **(B)** P-TDP-43 was similarly thresholded to exclude pixels detected in the no P-TDP-43 primary antibody control samples. **(C)** Using the Imaris Coloc function a new channel was generated that corresponded to the pixels (after thresholding) that were in present in both the PHF-1 and P-TDP-43 channel. The merged image of the channels is shown in **(D)**. **(E)** A

surface reconstruction was generated for the PHF-1 and P-TDP-43 to unbiasedly count the number of cell (PHF-1) and inclusions (P-TDP-43) in each image. Note that the PHF-1 staining in **(A)** was below the size threshold to be counted as a cell, thus no surface was rendered for the PHF-1 inclusion. **(F)** Imaris spot detection function was used to count the total number of DAPI positive cells in images. The yellow spheres in the picture highlight the detection of individual DAPI positive cells using the spot detection function.

DISCUSSION

Our findings provide insights into patterns of protein misfolding that are associated with prevalent human brain diseases: AD and CARTS. Hippocampal TDP-43 pathology was increased with advanced AD – Braak NFT stages V/VI – compared with lower Braak NFT stages. By contrast, AGs did not appear to have a correlation with TDP-43 pathology in this sample. In CARTS cases, dentate granule NFTs were frequently observed, more than would be expected according to Braak NFT stages. Since dentate granule neurons harbor NFTs without comorbid AD, one could argue that CARTS may be categorized as a tauopathy, but one where the spread of tau NFTs differs from classic AD or primary age-related tauopathy which are graded according to the Braak NFT staging (14, 53).

There are limitations to this study. While the sample was drawn from a community-based cohort (71), the included cases represent a convenience subsample that had been stained for TDP-43 using

immunohistochemistry, and neuropathologic findings are not representative of a population-based cohort in terms of ethnicity and socioeconomic variables. In addition, we limited our analysis to the hippocampus, and the observed relationships may or may not have implications about other brain regions. Further technical limitations included the possibility of underestimating AG burden given that a specific 4R-immunostain was not utilized for AG detection (22, 23, 75). The reason we included the study of AGs in our study design is that other researchers have reported an overrepresentation of AG pathology in TDP-43[+] cases (5, 25). We note that in our autopsy cohort (55), as in others (35, 69), AGs were not associated with cognitive impairment independent of other pathologies, whereas AGs are associated with dementia in other cohorts (9, 30, 74). Thus, there may be a discrepancy between the diseases underlying AG pathology seen in various populations and/or autopsy cohorts. We also note that this sample size may have been too small to provide adequate statistical power to test the hypothesis that AGs and TDP-43 are associated with each other.

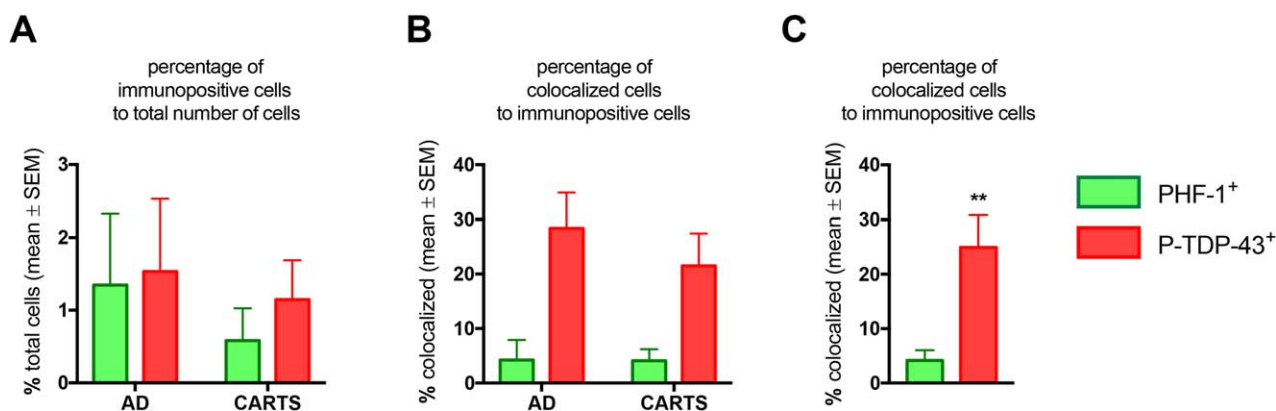


Figure 4. Results of counts and colocalization of PHF-1 and P-TDP-43 immunoreactive profiles in dentate granule neurons, in advanced AD (Braak NFT stages) and CARTS cases. This is the result of analyses of a subsample of 6 cases with 2 slides/case analyzed, comprising 14 200 dentate granule neurons from CARTS cases and 11 952 cells from AD cases. Panel A shows the overall percentage of immunopositive cells. Note that approximately 1% of cells are positive for PHF-1 and P-TDP-43, with trend for more PHF-1 immunoreactive cells in the

dentate granule cell layer from AD cases. Panel B shows the percentage of cells that are colocalized among those that are immunopositive. Panel C shows that in both AD and CARTS, a higher percentage (~25%) of cells that were TDP-43 immunopositive were also PHF-1 immunopositive, in comparison with the colocalization among the PHF-1 immunopositive cells in terms of P-TDP-43 immunopositivity (4%) ***P* = 0.007.

Despite these limitations, the analyses support two main findings: (i) We confirm prior results showing that TDP-43 pathology is more likely to occur in advanced AD as operationalized with Braak NFT stages V/VI (2, 17, 58, 66, 76, 79, 83); and (ii) We found that dentate granule neurons harbor NFTs in cases with comorbid hippocampal TDP-43 pathology but lacking advanced AD, that is CARTS. The latter finding could be used by neuropathologists as a proxy indicator of CARTS (see Figure 5).

CARTS is a highly prevalent disease (12, 19, 32, 46, 65, 83). For comparison's sake, an epidemiologic study found that the lifetime risk for developing FTLD is less than 1:700 in the United Kingdom (13), while a separate study predicted that FTLD affects 20 000–30 000 persons in the United States (40) – and these estimates included tauopathic FTLD. In sharp contrast, non-FTLD TDP-43 pathology affects ~1/3rd of elderly individuals in community-based cohorts (32, 39, 56), which would indicate that millions are impacted currently by non-FTLD TDP-43 pathology, and even more will be affected as the aged population expands. TDP-43 pathology in both CARTS and AD is consistently associated with cognitive impairment (37, 54, 55). The high prevalence and clinical impact of TDP-43 pathology in the aged population is commonly underappreciated.

A general point that is supported by our study is that the diagnostic term CARTS is *useful*. Without CARTS, the limitations of extant consensus-based diagnostic terminology lead to diagnostic dilemmas for neuropathologists. There are at least four challenges that a neuropathologist may face when performing an autopsy of an aged person with TDP-43 and/or HS pathologies: first, many brains harbor both AD and TDP-43 pathologies, and there is lack of a consensus-based classification scheme to assign the TDP-43 pathology as “belonging” to AD, HS, or both (20); second, TDP-43 pathology is present in many brains that lack full-blown AD or HS (4, 28, 54), and there is no consensus-based criteria for diagnosing the early (pre-HS) stages of the disease; third, focusing on HS itself is suboptimal, because extensive pathology (TDP-43 pathology

and/or atrophy) exists outside of the hippocampus in CARTS (39, 42, 54, 59, 62); and finally, the term HS is far more commonly applied in the literature to a completely different disease category – epilepsy. CARTS provides a terminology with criteria to surmount each of these challenges. Furthermore, we underscore that the usefulness of the term is even greater in the research setting to define cases and controls, and to enable testing of hypotheses related to this disease.

This study helps to clarify the “border region” between AD and CARTS pathologies. In AD, Braak NFT Stages V or VI indicate widespread tau pathology as visualized by a phospho-tau immunostain (8), such that by the time the dentate granule neurons are affected by NFTs, a substantial burden of pathology has accumulated. The CA1 region is affected earlier (from Braak NFT Stage III) in AD, when compared with the fascia dentata, which is not strongly involved until later stages (typically Braak NFT Stage V–VI) (8). By contrast, in CARTS, phospho-tau immunoreactivity is observed in the fascia dentata when there is minimal involvement of the CA1 region (Braak NFT Stages 0–II).

Prior studies found evidence in support of the hypothesis that proteins misfolded in neurodegenerative diseases may act synergistically or in parallel in the same cases. For example, in individuals with germline *APP* gene mutations, multiple different proteins become misfolded including Aβ, tau, α-synuclein, and TDP-43 (44, 47, 68). AD-type pathology (particularly Aβ plaques) are seen in α-synucleinopathy (31, 82), and co-aggregation of tau and α-synuclein has been reported in the locus coeruleus in progressive supranuclear palsy brains (21). Furthermore, α-synuclein inclusion bodies are common in the medial temporal lobe in the context of advanced AD pathology (5, 24, 64), again supportive of the hypothesis that multiple synergistic misfolded protein abnormalities can be present in end-stage AD. This study underscores that TDP-43 pathology is disproportionately common in advanced AD, so that if CARTS is a separate disease, it can only be diagnosed with confidence in cases with Braak NFT stage IV or lower as suggested

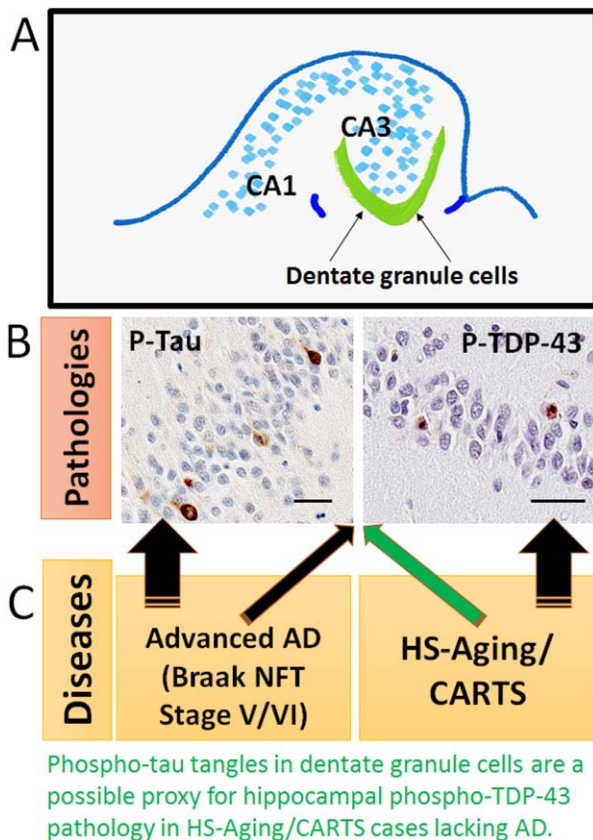


Figure 5. Hippocampal dentate granule NFTs are associated with advanced AD and also with the presence of TDP-43 pathology in low Braak stage (CARTS) cases. Schematic depiction of hippocampal formation (**A**) to show how the pathologies studied in the dentate granule neurons (**B**) are correlated with different common brain diseases (**C**). Both phospho-Tau and phospho-TDP-43 pathologies commonly occur in both advanced AD and in CARTS. This implies that disparate upstream causal factors may lead to common downstream pathologic pathways. The appearance of dentate granule NFTs in cases without AD pathology may serve as a useful proxy for indicating CARTS (green arrow). Both of these particular brightfield photomicrographs were taken from the same CARTS case, counterstained with hematoxylin; scale bars = 40 μ M.

previously (60). However, the biologic mechanisms underlying CARTS could be present in some cases with comorbid advanced AD, only masked, highlighting the need for more specific disease biomarkers.

We conclude that CARTS and AD are each brain diseases where autopsy may reveal both TDP-43 and tau pathologies, albeit associated with different genetic risk factors, anatomic distribution of the neuropathologic lesions, and clinical outcomes. TDP-43 pathology could be exacerbated by tau pathology, or vice versa, or the two could be mutually synergistic. Alternatively, TDP-43 pathology may occur in parallel with tauopathy, secondary to common “upstream” pathogenetic factor(s). Although our cross-sectional study cannot deduce a mechanism, there is a potential practical benefit to this observation: in the absence of advanced AD pathology, neuropathologists can use dentate granule phospho-tau

immunostain as a proxy indicator of CARTS (Figure 5), but this should still be confirmed with TDP-43 immunostain.

ACKNOWLEDGMENTS

We are deeply grateful to the study participants and clinicians who made this research possible. The authors thank Sonya Anderson and Ela Patel for technical support. Study funding: P30 AG028383 from the National Institutes of Health. Thanks also to Dr. Peter Davies (PHF-1) and Dr. Manuela Neumann (1D3) for generously providing antibody. The corresponding author Dr. Peter Nelson had full access to all of the data in the study and takes responsibility for the integrity of the data and the accuracy of the data analysis.

REFERENCES

1. Abisambra JF, Scheff S (2014) Brain injury in the context of tauopathies. *J Alzheimer's Dis* **40**:495–518.
2. Amador-Ortiz C, Ahmed Z, Zehr C, Dickson DW (2007) Hippocampal sclerosis dementia differs from hippocampal sclerosis in frontal lobe degeneration. *Acta Neuropathol* **113**:245–252.
3. Amador-Ortiz C, Lin WL, Ahmed Z, Personett D, Davies P, Duara R *et al* (2007) TDP-43 immunoreactivity in hippocampal sclerosis and Alzheimer's disease. *Ann Neurol* **61**:435–445.
4. Aoki N, Murray ME, Ogaki K, Fujioka S, Rutherford NJ, Rademakers R *et al* (2015) Hippocampal sclerosis in Lewy body disease is a TDP-43 proteinopathy similar to FTLN-TDP Type A. *Acta Neuropathol* **129**:53–64.
5. Arnold SJ, Dugger BN, Beach TG (2013) TDP-43 deposition in prospectively followed, cognitively normal elderly individuals: correlation with argyrophilic grains but not other concomitant pathologies. *Acta Neuropathol* **126**:51–57.
6. Bachstetter AD, Van Eldik LJ, Schmitt FA, Neltner JH, Ighodaro ET, Webster SJ *et al* (2015) Disease-related microglia heterogeneity in the hippocampus of Alzheimer's disease, dementia with Lewy bodies, and hippocampal sclerosis of aging. *Acta Neuropathol Commun* **3**:32–48.
7. Beach TG, Sue L, Scott S, Layne K, Newell A, Walker D *et al* (2003) Hippocampal sclerosis dementia with tauopathy. *Brain Pathol* **13**:263–278.
8. Braak H, Alafuzoff I, Arzberger T, Kretschmar H, Del Tredici K (2006) Staging of Alzheimer disease-associated neurofibrillary pathology using paraffin sections and immunocytochemistry. *Acta Neuropathol* **112**:389–404.
9. Braak H, Braak E (1989) Cortical and subcortical argyrophilic grains characterize a disease associated with adult onset dementia. *Neuropathol Appl Neurobiol* **15**:13–26.
10. Brenowitz WD, Monsell SE, Schmitt FA, Kukull WA, Nelson PT (2014) Hippocampal sclerosis of aging is a key Alzheimer's disease mimic: clinical-pathologic correlations and comparisons with both Alzheimer's disease and non-tauopathic frontotemporal lobar degeneration. *J Alzheimer's Dis* **39**:691–702.
11. Corey-Bloom J, Sabbagh MN, Bondi MW, Hansen L, Alford MF, Masliah E, Thal LJ (1997) Hippocampal sclerosis contributes to dementia in the elderly. *Neurology* **48**:154–160.
12. Corrada MM, Berlau DJ, Kawas CH (2012) A population-based clinicopathological study in the oldest-old: the 90+ study. *Curr Alzheimer Res* **9**:709–717.
13. Coyle-Gilchrist IT, Dick KM, Patterson K, Vazquez Rodriguez P, Wehmann E, Wilcox A *et al* (2016) Prevalence, characteristics, and survival of frontotemporal lobar degeneration syndromes. *Neurology* **86**:1736–1743.

14. Crary JF, Trojanowski JQ, Schneider JA, Abisambra JF, Abner EL, Alafuzoff I *et al* (2014) Primary age-related tauopathy (PART): a common pathology associated with human aging. *Acta Neuropathol* **128**:755–766.
15. Cykowski MD, Powell SZ, Schulz PE, Takei H, Rivera AL, Jackson R *et al*. Hippocampal sclerosis in older patients: practical examples and guidance with a focus on cerebral age-related TDP-43 with sclerosis (CARTS). *Arch Pathol Lab Med* (in press).
16. Cykowski MD, Takei H, Van Eldik LJ, Schmitt FA, Jicha GA, Powell SZ, Nelson PT (2016) Hippocampal sclerosis but not normal aging or Alzheimer disease is associated with TDP-43 pathology in the basal forebrain of aged persons. *J Neuropathol Exp Neurol* **75**:397–407.
17. Davidson YS, Raby S, Foulds PG, Robinson A, Thompson JC, Sikkink S *et al* (2011) TDP-43 pathological changes in early onset familial and sporadic Alzheimer's disease, late onset Alzheimer's disease and Down's syndrome: association with age, hippocampal sclerosis and clinical phenotype. *Acta Neuropathol* **122**:703–713.
18. Davis DG, Schmitt FA, Wekstein DR, Markesbery WR (1999) Alzheimer neuropathologic alterations in aged cognitively normal subjects. *J Neuropathol Exp Neurol* **58**:376–388.
19. Dickson DW, Davies P, Bevona C, Van Hoesven KH, Factor SM, Grober E *et al* (1994) Hippocampal sclerosis: a common pathological feature of dementia in very old (> or = 80 years of age) humans. *Acta Neuropathol* **88**:212–221.
20. Dutra JR, Cortes EP, Vonsattel JP (2015) Update on hippocampal sclerosis. *Curr Neurol Neurosci Rep* **15**:67–76.
21. Erro Aguirre ME, Zelaya MV, Sanchez Ruiz de Gordo J, Tunon MT, Lanciego JL (2015) Midbrain catecholaminergic neurons co-express alpha-synuclein and tau in progressive supranuclear palsy. *Front Neuroanat* **9**:25–33.
22. Ferrer I, Santpere G, van Leeuwen FW (2008) Argyrophilic grain disease. *Brain* **131**:1416–1432.
23. Fujino Y, Wang DS, Thomas N, Espinoza M, Davies P, Dickson DW (2005) Increased frequency of argyrophilic grain disease in Alzheimer disease with 4R tau-specific immunohistochemistry. *J Neuropathol Exp Neurol* **64**:209–214.
24. Fujishiro H, Tsuboi Y, Lin WL, Uchikado H, Dickson DW (2008) Co-localization of tau and alpha-synuclein in the olfactory bulb in Alzheimer's disease with amygdala Lewy bodies. *Acta Neuropathol* **116**:17–24.
25. Fujishiro H, Uchikado H, Arai T, Hasegawa M, Akiyama H, Yokota O *et al* (2009) Accumulation of phosphorylated TDP-43 in brains of patients with argyrophilic grain disease. *Acta Neuropathol* **117**:151–158.
26. Goedert M (2016) The ordered assembly of tau is the gain-of-toxic function that causes human tauopathies. *Alzheimer's Dement* **12**:1040–1050.
27. Higashi S, Iseki E, Yamamoto R, Minegishi M, Hino H, Fujisawa K *et al* (2007) Concurrence of TDP-43, tau and alpha-synuclein pathology in brains of Alzheimer's disease and dementia with Lewy bodies. *Brain Res* **1184**:284–294.
28. Ighodaro ET, Jicha GA, Schmitt FA, Neltner JH, Abner EL, Kryscio RJ *et al* (2015) Hippocampal sclerosis of aging can be segmental: two cases and review of the literature. *J Neuropathol Exp Neurol* **74**:642–652.
29. Iguchi Y, Katsuno M, Takagi S, Ishigaki S, Niwa J, Hasegawa M *et al* (2012) Oxidative stress induced by glutathione depletion reproduces pathological modifications of TDP-43 linked to TDP-43 proteinopathies. *Neurobiol Dis* **45**:862–870.
30. Ikeda K (2008) Clinical aspects of dementia with argyrophilic grains. *Handb Clin Neurol* **89**:549–552.
31. Irwin DJ, Lee VM, Trojanowski JQ (2013) Parkinson's disease dementia: convergence of alpha-synuclein, tau and amyloid-beta pathologies. *Nat Rev Neurosci* **14**:626–636.
32. James BD, Wilson RS, Boyle PA, Trojanowski JQ, Bennett DA, Schneider JA (2016) TDP-43 stage, mixed pathologies, and clinical Alzheimer's-type dementia. *Brain* [Epub ahead of print].
33. Josephs KA, Murray ME, Whitwell JL, Tosakulwong N, Weigand SD, Petrucelli L *et al* (2016) Updated TDP-43 in Alzheimer's disease staging scheme. *Acta Neuropathol* **131**:571–585.
34. Josephs KA, Whitwell JL, Knopman DS, Hu WT, Stroh DA, Baker M *et al* (2008) Abnormal TDP-43 immunoreactivity in AD modifies clinicopathologic and radiologic phenotype. *Neurology* **70**:1850–1857.
35. Josephs KA, Whitwell JL, Parisi JE, Knopman DS, Boeve BF, Geda YE *et al* (2008) Argyrophilic grains: a distinct disease or an additive pathology? *Neurobiol Aging* **29**:566–573.
36. Josephs KA, Whitwell JL, Tosakulwong N, Weigand SD, Murray ME, Liesinger AM *et al* (2015) TAR DNA-binding protein 43 and pathological subtype of Alzheimer's disease impact clinical features. *Ann Neurol* **78**:697–709.
37. Josephs KA, Whitwell JL, Weigand SD, Murray ME, Tosakulwong N, Liesinger AM *et al* (2014) TDP-43 is a key player in the clinical features associated with Alzheimer's disease. *Acta Neuropathol* **127**:811–824.
38. Kadokura A, Yamazaki T, Lemere CA, Takatama M, Okamoto K (2009) Regional distribution of TDP-43 inclusions in Alzheimer disease (AD) brains: their relation to AD common pathology. *Neuropathology* **29**:566–573.
39. Keage HA, Hunter S, Matthews FE, Ince PG, Hodges J, Hokkanen SR *et al* (2014) TDP-43 pathology in the population: prevalence and associations with dementia and age. *J Alzheimer's Dis* **42**:641–650.
40. Knopman DS, Roberts RO (2011) Estimating the number of persons with frontotemporal lobar degeneration in the US population. *J Mol Neurosci* **45**:330–335.
41. Koga S, Sanchez-Contreras M, Josephs KA, Uitti RJ, Graff-Radford N, van Gerpen JA, *et al* (2016) Distribution and characteristics of transactive response DNA binding protein 43 kDa pathology in progressive supranuclear palsy. *Mov Disord* [Epub ahead of print].
42. Kotrotsou A, Schneider JA, Bennett DA, Leurgans SE, Dawe RJ, Boyle PA *et al* (2015) Neuropathologic correlates of regional brain volumes in a community cohort of older adults. *Neurobiol Aging* **36**:2798–2805.
43. Kovacs GG (2016) Molecular pathological classification of neurodegenerative diseases: turning towards precision medicine. *Int J Mol Sci* **17**:1–33.
44. Kraybill ML, Larson EB, Tsuang DW, Teri L, McCormick WC, Bowen JD *et al* (2005) Cognitive differences in dementia patients with autopsy-verified AD, Lewy body pathology, or both. *Neurology* **64**:2069–2073.
45. Kryscio RJ, Abner EL, Jicha GA, Nelson PT, Smith CD, Van Eldik LJ *et al* (2016) Self-reported memory complaints: a comparison of demented and unimpaired outcomes. *J Prev Alzheimer's Dis* **3**:13–19.
46. Leverenz JB, Agustin CM, Tsuang D, Peskind ER, Edland SD, Nochlin D *et al* (2002) Clinical and neuropathological characteristics of hippocampal sclerosis: a community-based study. *Arch Neurol* **59**:1099–1106.
47. Lippa CF, Fujiwara H, Mann DM, Giasson B, Baba M, Schmidt ML *et al* (1998) Lewy bodies contain altered alpha-synuclein in brains of many familial Alzheimer's disease patients with mutations in presenilin and amyloid precursor protein genes. *Am J Pathol* **153**:1365–1370.
48. McAleese KE, Walker L, Erskine D, Thomas AJ, McKeith IG, Attems J (2016) TDP-43 pathology in Alzheimer's disease, dementia with Lewy bodies, and ageing. *Brain Pathol* [Epub ahead of print].
49. McKee AC, Gavett BE, Stem RA, Nowinski CJ, Cantu RC, Kowall NW *et al* (2010) TDP-43 proteinopathy and motor neuron disease in chronic traumatic encephalopathy. *J Neuropathol Exp Neurol* **69**:918–929.
50. McKhann GM, Knopman DS, Chertkow H, Hyman BT, Jack CR Jr, Kawas CH *et al* (2011) The diagnosis of dementia due to Alzheimer's

- disease: recommendations from the National Institute on Aging-Alzheimer's Association workgroups on diagnostic guidelines for Alzheimer's disease. *Alzheimer's Dementia* **7**:263–269.
51. Miki Y, Mori F, Hori E, Kaimori M, Wakabayashi K (2009) Hippocampal sclerosis with four-repeat tau-positive round inclusions in the dentate gyrus: a new type of four-repeat tauopathy. *Acta Neuropathol* **117**:713–718.
 52. Mirra SS, Heyman A, McKeel D, Sumi SM, Crain BJ, Brownlee LM *et al* (1991) The consortium to establish a registry for Alzheimer's disease (CERAD). Part II. Standardization of the neuropathologic assessment of Alzheimer's disease. *Neurology* **41**: 479–486.
 53. Montine TJ, Phelps CH, Beach TG, Bigio EH, Cairns NJ, Dickson DW, *et al* (2012) National Institute on Aging-Alzheimer's Association guidelines for the neuropathologic assessment of Alzheimer's disease: a practical approach. *Acta Neuropathol* **123**:1–11.
 54. Nag S, Yu L, Capuano AW, Wilson RS, Leurgans SE, Bennett DA, Schneider JA (2015) Hippocampal sclerosis and TDP-43 pathology in aging and Alzheimer disease. *Ann Neurol* **77**:942–952.
 55. Nelson PT, Abner EL, Schmitt FA, Kryscio RJ, Jicha GA, Smith CD *et al* (2010) Modeling the association between 43 different clinical and pathological variables and the severity of cognitive impairment in a large autopsy cohort of elderly persons. *Brain Pathol* **20**:66–79.
 56. Nelson PT, Head E, Schmitt FA, Davis PR, Neltner JH, Jicha GA *et al* (2011) Alzheimer's disease is not "brain aging": neuropathological, genetic, and epidemiological human studies. *Acta Neuropathol* **121**: 571–587.
 57. Nelson PT, Jicha GA, Schmitt FA, Liu H, Davis DG, Mendiondo MS *et al* (2007) Clinicopathologic correlations in a large Alzheimer disease center autopsy cohort: neuritic plaques and neurofibrillary tangles "do count" when staging disease severity. *J Neuropathol Exp Neurol* **66**: 1136–1146.
 58. Nelson PT, Schmitt FA, Lin Y, Abner EL, Jicha GA, Patel E *et al* (2011) Hippocampal sclerosis in advanced age: clinical and pathological features. *Brain* **134**:1506–1518.
 59. Nelson PT, Smith CD, Abner EL, Wilfred BJ, Wang WX, Neltner JH *et al* (2013) Hippocampal sclerosis of aging, a prevalent and high-morbidity brain disease. *Acta Neuropathol* **126**:161–177.
 60. Nelson PT, Trojanowski JQ, Abner EL, Al-Janabi OM, Jicha GA, Schmitt FA *et al* (2016) "New Old Pathologies": AD, PART, and cerebral age-related TDP-43 with sclerosis (CARTS). *J Neuropathol Exp Neurol* **75**:482–498.
 61. Neumann M, Sampathu DM, Kwong LK, Truax AC, Micsenyi MC, Chou TT *et al* (2006) Ubiquitinated TDP-43 in frontotemporal lobar degeneration and amyotrophic lateral sclerosis. *Science* **314**:130–133.
 62. Nho K, Saykin AJ, Alzheimer's Disease Neuroimaging I, Nelson PT (2016) Hippocampal sclerosis of aging, a common Alzheimer's disease 'Mimic': risk genotypes are associated with brain atrophy outside the temporal lobe. *J Alzheimer's Dis* **52**:373–383.
 63. Pao WC, Dickson DW, Crook JE, Finch NA, Rademakers R, Graff-Radford NR (2011) Hippocampal sclerosis in the elderly: genetic and pathologic findings, some mimicking Alzheimer disease clinically. *Alzheimer Dis Assoc Disord* **25**:364–368.
 64. Popescu A, Lippa CF, Lee VM, Trojanowski JQ (2004) Lewy bodies in the amygdala: increase of alpha-synuclein aggregates in neurodegenerative diseases with tau-based inclusions. *Arch Neurol* **61**: 1915–1919.
 65. Rauramaa T, Pikkarainen M, Englund E, Ince PG, Jellinger K, Paetau A, Alafuzoff I (2011) TAR-DNA binding protein-43 and alterations in the hippocampus. *J Neural Transm* **118**:683–689.
 66. Rauramaa T, Pikkarainen M, Englund E, Ince PG, Jellinger K, Paetau A, Alafuzoff I (2013) Consensus recommendations on pathologic changes in the hippocampus: a postmortem multicenter inter-rater study. *J Neuropathol Exp Neurol* **72**:452–461.
 67. Riley KP, Snowden DA, Markesbery WR (2002) Alzheimer's neurofibrillary pathology and the spectrum of cognitive function: findings from the Nun Study. *Ann Neurol* **51**:567–577.
 68. Rosenberg CK, Pericak-Vance MA, Saunders AM, Gilbert JR, Gaskell PC, Hulette CM (2000) Lewy body and Alzheimer pathology in a family with the amyloid-beta precursor protein APP717 gene mutation. *Acta Neuropathol* **100**:145–152.
 69. Sabbagh MN, Sandhu SS, Farlow MR, Vedders L, Shill HA, Caviness JN *et al* (2009) Correlation of clinical features with argyrophilic grains at autopsy. *Alzheimer Dis Assoc Disord* **23**:229–233.
 70. Saing T, Dick M, Nelson PT, Kim RC, Cribbs DH, Head E (2012) Frontal cortex neuropathology in dementia pugilistica. *J Neurotrauma* **29**:1054–1070.
 71. Schmitt FA, Nelson PT, Abner E, Scheff S, Jicha GA, Smith C *et al* (2012) University of Kentucky Sanders-Brown healthy brain aging volunteers: donor characteristics, procedures and neuropathology. *Curr Alzheimer Res* **9**:724–733.
 72. Schmitt FA, Wetherby MM, Wekstein DR, Dearth CM, Markesbery WR (2001) Brain donation in normal aging: procedures, motivations, and donor characteristics from the Biologically Resilient Adults in Neurological Studies (BRAiNS) Project. *Gerontologist* **41**:716–722.
 73. Spillantini MG, Goedert M (2013) Tau pathology and neurodegeneration. *Lancet Neurol* **12**:609–622.
 74. Steuerwald GM, Baumann TP, Taylor KI, Mittag M, Adams H, Tolnay M, Monsch AU (2007) Clinical characteristics of dementia associated with argyrophilic grain disease. *Dement Geriatr Cogn Disord* **24**:229–234.
 75. Togo T, Cookson N, Dickson DW (2002) Argyrophilic grain disease: neuropathology, frequency in a dementia brain bank and lack of relationship with apolipoprotein E. *Brain Pathol* **12**:45–52.
 76. Tremblay C, St-Amour I, Schneider J, Bennett DA, Calon F (2011) Accumulation of transactive response DNA binding protein 43 in mild cognitive impairment and Alzheimer disease. *J Neuropathol Exp Neurol* **70**:788–798.
 77. Tsuji H, Arai T, Kametani F, Nonaka T, Yamashita M, Suzukake M *et al* (2012) Molecular analysis and biochemical classification of TDP-43 proteinopathy. *Brain* **135**:3380–3391.
 78. Uchino A, Takao M, Hatsuta H, Sumikura H, Nakano Y, Nogami A *et al* (2015) Incidence and extent of TDP-43 accumulation in aging human brain. *Acta Neuropathol Commun* **3**:35–46.
 79. Wilson AC, Dugger BN, Dickson DW, Wang DS (2011) TDP-43 in aging and Alzheimer's disease – a review. *Int J Clin Exp Pathol* **4**: 147–155.
 80. Wolf DS, Gearing M, Snowden DA, Mori H, Markesbery WR, Mirra SS (1999) Progression of regional neuropathology in Alzheimer disease and normal elderly: findings from the Nun study. *Alzheimer Dis Assoc Disord* **13**:226–231.
 81. Yokota O, Davidson Y, Arai T, Hasegawa M, Akiyama H, Ishizu H *et al* (2010) Effect of topographical distribution of alpha-synuclein pathology on TDP-43 accumulation in Lewy body disease. *Acta Neuropathol* **120**:789–801.
 82. Zaccai J, Brayne C, McKeith I, Matthews F, Ince PG, Mrc Cognitive Function ANS (2008) Patterns and stages of alpha-synucleinopathy: relevance in a population-based cohort. *Neurology* **70**:1042–1048.
 83. Zarow C, Weiner MW, Ellis WG, Chui HC (2012) Prevalence, laterality, and comorbidity of hippocampal sclerosis in an autopsy sample. *Brain Behav* **2**:435–442.